Comparison of the Electrical Resistance and Potential Techniques for the Self-sensing of Damage in Carbon Fiber Polymer-Matrix Composites

Daojun Wang, Shoukai Wang, D. D. L. Chung and Jaycee H. Chung

Journal of Intelligent Material Systems and Structures 2006; 17; 853
DOI: 10.1177/1045389X06060218

Comparison of the Electrical Resistance and Potential Techniques for the Self-sensing of Damage in Carbon Fiber Polymer–Matrix Composites

DAOJUN WANG,[1] SHOUKAI WANG,[1] D. D. L. CHUNG[1,*] AND JAYCEE H. CHUNG[2]

[1]*Composite Materials Research Laboratory, University at Buffalo, State University of New York Buffalo, NY 14260-4400, USA*

[2]*Global Contour Ltd, 1145 Ridge Road West, Rockwall, TX 75087, USA*

ABSTRACT: The electric potential method, which involves measuring the potential at a distance from the line of current application, is effective for damage sensing of carbon fiber polymer–matrix composites when the distance is sufficiently small, such as 1.0 mm (8 laminae) in the through-thickness direction. It is ineffective when this distance is 2.1 mm (16 laminae). The electrical resistance method, which involves measuring the potential on the line of current application, has no thickness limitation. However, it suffers from current path distortion upon damage and the consequent reduced sensitivity for damage. A minor phenomenon of the measured resistance decreasing with increasing damage is observed for the regions of the composite not containing the point of impact. The major phenomenon of the resistance increasing with damage overshadows this minor phenomenon for the region containing the point of impact.

Key Words: electric potential, electrical resistance, sensing, damage, composite, carbon fiber, polymer.

INTRODUCTION

DUE to aging, lightning, impact, and other causes, aircraft suffer from structural damage which may or may not be visible (Wolterman, et al., 1993; Shin et al., 1995; Chung and Seferis, 1998). In the case of the structural material being a carbon fiber polymer-matrix composite, which is attractive for its combination of high stiffness, high strength and low density, the damage can be in the form of delamination (local separation between the layers of fibers in the composite, which comprises typically tens of fiber layers), fiber-matrix debonding, and fiber breakage (Shin et al., 1996). A fiber layer, also known as a lamina, is typically thousands of fibers in thickness, as each fiber tow consists of thousands of fibers. Delamination is the most common form of damage. As the delamination can occur between the interior laminae of a composite, delamination is commonly not visible at the surface of the composite.

Fiber-matrix debonding, which occurs locally, can be due to the inadequate adhesion between fiber and matrix and thermal expansion mismatch between fiber and matrix. This mismatch is inevitable, as carbon fiber has a much lower value of the thermal expansion coefficient than polymers. Upon temperature variation, as commonly encountered due to the difference in temperature between ground and air, the thermal expansion mismatch results in thermal fatigue. Fiber–matrix debonding is a relatively subtle form of damage that is not usually visible at the surface of the composite.

Fiber breakage is a form of damage which typically occurs when the damage is extensive. If the fibers that are broken are at the surface of the composite, fiber breakage can be visible at the surface; otherwise, it is not visible.

Ultrasonic inspection (Rose et al., 1996; de Freitas et al., 2000; Sjogren, et al., 2001) is a nondestructive method for detecting damage in the form of subsurface cracks that are lateral size of at least about 1 mm; the higher the frequency of the ultrasonic wave, the better is the ability to detect small cracks. Thus, ultrasonic inspection is effective for detecting delamination that is of sufficient size in the plane of the delamination. For delamination cracks that are insufficiently large in size or are not welldeveloped (due to the infancy of the delamination), ultrasonic inspection is not effective. X-radiography (Avier and Clarke, 1995) is another nondestructive method for damage detection, but its ability to detect small flaws is worse than that of

*Author to whom correspondence should be addressed.
E-mail: ddlchung@buffalo.edu
Figure 2 appears in color online: http://jim.sagepub.com

1045-389X/06/10 0853–9 $10.00/0 DOI: 10.1177/1045389X06060218

ultrasonic inspection. Yet another nondestructive method is acoustic emission (Clerico et al., 1989; Verma, et al., 1994; Haque and Raju, 1998), which is limited to the detection of damage during (not after) the occurrence of damage. The method involving strain or flexibility measurement for damage detection (Aoki and Byon, 2001) may not be totally nondestructive, due to the stress applied to the composite. The embedment of optical fibers (Staszewski et al., 1999) for damage detection is of concern, due to the sites of stress concentration that are associated with the embedded optical fibers and due to the difficulty of repair.

Electrical measurement is a method of nondestructive evaluation. It can be in the form of electrical resistance measurement, as the resistance is changed upon damage (Prabhakaran, 1990; Muto et al., 1992, 1995; Schulte, 1993; Kaddour et al., 1994; Sugita et al., 1995; Todoroki et al., 1995; Ceysson et al., 1996; Irving and Thiagarajan, 1998; Wang et al., 1998a, b; Wang and Chung, 1999; Wang et al., 1999; Abry et al., 1999, 2001; Chu and Yum, 2001; Kupke et al., 2001; Wang et al., 2001; Mei et al., 2002; Wang and Chung, 2002; Chung and Wang, 2003; Wang et al., 2004; Yoshitake et al., 2004). As a consequence, the change in resistance provides an indication of the extent of damage. Furthermore, the resistance distribution provides an indication of the damage distribution (Chung and Wang, 2003; Wang et al., 2004; Wang et al., 2005, in press (a). The through-thickness resistance of a composite is increased upon delamination, because the extent of contact between fibers of adjacent laminae is diminished by delamination (Chung and Wang, 2003). The longitudinal resistance (i.e., resistance in the fiber direction) is increased upon fiber breakage (Wang and Chung, 1999). Thus, by measuring the resistance in different directions, different types of damage can be detected.

Related to, but distinct from, the method of electrical resistance measurement is that of electric potential measurement (Masson and Irving, 2000; Todoroki et al., 2004; Angelidis et al., 2005). In the electrical resistance method, the current path and the potential gradient path coincide. In contrast, in the electric potential method, the two paths in general do not coincide. Furthermore, in the resistance method, the current used typically decreases with increasing resistance in a way that is set by the resistance meter, so that the current is not fixed. Alternatively, the current may be fixed in the resistance method. In contrast, in the potential method, the current is necessarily fixed; with a fixed current between two chosen points on the surface of the composite, the potential (say, relative to the electrical ground) is measured at various other points on the composite surface, or the potential difference is measured for various pairs of other points on the composite surface. Thus, in the potential method, the points for current application are in general not in line with those for potential measurement. The difference in potential between two points relates to the resistance between these points, but the relationship is not simple when the current path and potential gradient path do not coincide.

In the method of electric potential measurement, the meaning of the potential of a particular point is ambiguous, as the change in potential of a particular point depends on the condition in the vicinity of the point and cannot imply the occurrence of damage at this point. The meaning of the potential difference between two points is less ambiguous than the potential at a particular point, due to its having a degree of relationship with the resistance. However, the potential technique is attractive in that the measurement of the potential at a particular point can be made with a single electrical contact (in addition to the two current contacts). In contrast, the measurement of the resistance at a particular point requires two electrical contacts (in addition to the two current contacts, in case of the four-probe method, which is preferred to the two-probe method due to the exclusion of the contact resistance from the measured resistance). Due to the single electrical contact, the potential technique can provide more resolution in spatial distribution sensing than resistance measurement.

The potential distribution, as displayed in the form of two-dimensional equipotential contours, has been shown to provide two-dimensional damage distribution when the damage is substantial, e.g., damage inflicted by impact at energy 4 J or above (Angelidis et al., 2005) and damage corresponding to a delamination size of at least 10 mm (Todoroki et al., 2004). The ineffectiveness of the potential method to provide the damage distribution in the case of minor damage is due to the fact that the low electrical resistivity in the plane of the fibers causes the potential to spread (i.e., be smeared) in this plane (Angelidis et al., 2005; Wang et al., in press (b)). Even in the case of major damage, the spatial resolution of the damage sensing was ± 10 mm (Todoroki et al., 2004). It has been reported that there is no simple relation between the location of delamination and the measured potential distribution (Masson and Irving, 2000).

This article provides a comparative study of the electric potential and resistance methods, as used for damage distribution sensing in carbon fiber polymer-matrix composites. The comparison involves (i) measurement of the surface resistance by having the two current contacts in line with the two potential contacts and (ii) measurement of the surface potential by having the two current contacts not in line with the two potential contacts (such that the line joining the current contacts is parallel to that joining the potential contacts). Two configurations of resistance measurement were used to provide measurement of the top

surface resistance and the bottom surface resistance upon impact at the top surface, as illustrated in Figure 1(a) and (b), respectively. Two configurations of potential measurement were used to provide measurement of the bottom surface potential difference during top surface current application and of the top surface potential difference during bottom surface current application, as illustrated in Figure 1(c) and (d), respectively.

The objectives of the study are to: (i) compare the resistance and potential methods in terms of their effectiveness for damage sensing and spatial distribution sensing, (ii) determine the relationship between damage severity and electrical response, and (iii) compare composites of different thicknesses in terms of their suitability for selfsensing using the configurations of Figure 1. The relationship mentioned in (ii) has not been addressed explicitly in the prior work on damage distribution sensing using the electric potential method, due to the emphasis of prior work (Masson and Irving, 2000; Todoroki et al., 2004; Angelidis et al., 2005) on damage location determination rather than on damage severity determination.

This article addresses the potential method in which the potential is measured at a distance in the through-thickness direction from the line of current application. This configuration is relevant to the practical use of the method, as implementation of the method can involve applying the current on one surface of the laminate and measuring the potential at the opposite surface. In contrast, the potential method used in prior work involved the potential being measured at a distance in the plane of the fibers from the line of current application. Comparison of the resistance and potential methods for the in-plane (two-dimensional) case is the subject for a separate paper.

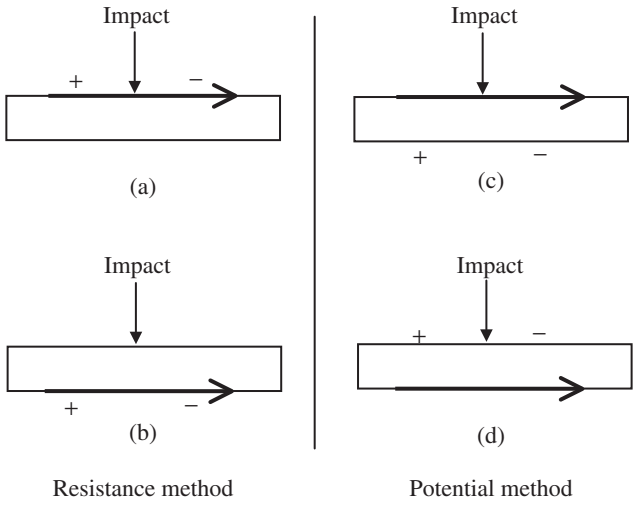

Figure 1. *Edge view of composite showing the configurations for resistance and potential measurements. Impact is directed at the center of the top surface. The thick arrow indicates the current: (a) top surface resistance measurement; (b) bottom surface resistance measurement; (c) bottom surface potential measurement (with current on the top surface); and (d) top surface potential measurement (with current on the bottom surface).*

EXPERIMENTAL METHODS

Commercially manufactured composites in the form of continuous carbon fiber epoxy-matrix laminates were cut into strips of size 200×12 mm and then lightly sanded by using 600 grit silicon carbide sand paper for the purpose of removing the surface layer (about 20 μm thick) of epoxy matrix prior to the application of electrical contacts. The contacts were in the form of silver paint in conjunction with copper wire. The sanding step is not essential, but it helps the electrical measurement by increasing the accuracy and decreasing the noise. Although the entire surface was sanded in this work, only the portions beneath the electrical contacts needed to be sanded.

Three laminates were studied, namely a 8-lamina quasi-isotropic $[0/45/90/-45]_s$ laminate (thickness = 1.0 mm), a 16-lamina quasi-isotropic $[0/45/90/-45]_{2s}$ laminate (thickness = 2.1 mm), and a 24-lamina quasi-isotropic $[0/45/90/-45]_{3s}$ laminate (thickness = 3.2 mm). For each specimen, the 0° direction was along the length of the specimen. In other words, the fibers of the top and bottom laminae were along the length of each specimen.

Eight electrical contacts were applied on each of the two large opposite sides of a laminate, as illustrated in

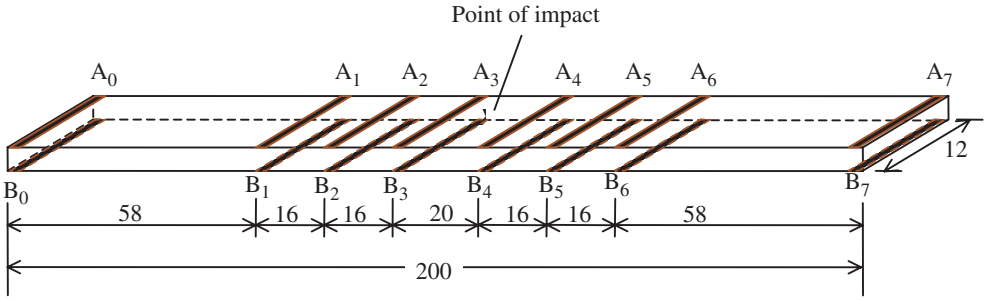

Figure 2. *Composite specimen testing configuration. Contacts $A_0, A_1, A_2, \ldots, A_7$ are on the top side of the specimen. Contacts $B_0, B_1, B_2, \ldots, B_7$ are on the bottom side, such that B_0 is directly opposite A_0, B_1 is directly opposite A_1, etc. The point of impact is on the top side at the center of the specimen along its 200 mm length. All dimensions are in mm.*

Figure 2. The outer two contacts on each surface are for passing current (i.e., A_0 and A_7 on the top surface and B_0 and B_7 on the bottom surface). The remaining contacts are for potential measurement. Six potential contacts on each side, with two adjacent ones used at a time, allow measurement of the potential difference across five regions. Each contact was in the form of a line along the entire 12 mm width of the specimen. The point of impact was at the center along the specimen length.

A constant current (100 mA) was used in conjunction with a Keithley 2002 multimeter for voltage measurement with a voltage limit of 50 V.

Damage was inflicted in this work by drop impact. The damage was much more localized than that inflicted by flexure.

Before and after impact, using a steel hemisphere (19 mm or 0.75″ diameter) dropped from a controlled height, potential measurements were made. The impact energy was calculated from the weight of the ball assembly (either 0.740 or 2.640 kg) and the initial height of the ball (up to 850 mm). The impact was directed at the same point of the specimen at progressively increasing energy. Hence, cumulative damage was analyzed. Although the cumulative damage is more than the damage resulting from a single impact at the maximum impact energy used in inflicting cumulative damage, it is meaningful in providing the damage evolution for the same specimen as the impact energy progressively increased.

Impact resulted in local and shallow indentation at and around the point of impact. For example, for the 8-lamina composite, the depth of the indentation was 0.26 mm after a single impact at 5.78 J; for the 24-lamina composite, the depth of the indentation was 0.20 mm after a single impact at 5.08 J (Wang et al., 2005). The depth of indentation increased with increasing impact energy.

The effect of such impact damage on the electrical resistance and its one-dimensional spatial distribution has been previously studied in (Wang et al., 2005). The study showed that the resistance distribution related to the damage distribution, though the study was limited to three segments of a specimen, i.e., the segment containing the point of impact, and the two segments flanking this segment. In contrast, this article addresses the effects of impact damage on the potential gradient (i.e., potential difference divided by the distance of separation of the potential contacts) of each segment, in addition to addressing the effect of impact damage on the resistance of each segment. There are five segments, i.e., the one segment containing the point of impact (segment between A_3 and A_4 in Figure 2), two segments to the left of this segment (segment between A_2 and A_3, and that between A_1 and A_2), and two segments to the right of this segment (segment between A_4 and A_5 and that between A_5 and A_6 in Figure 2).

The data shown in this article are representative specimens of each laminate. However, the general reproducibility of the results has been confirmed by testing three specimens of each type.

RESULTS AND DISCUSSION

8-Lamina Composite

Figures 3–6 show the results obtained for the 8-lamina composite using the configurations of Figure 1(a)–(d). Each figure shows the fractional change in potential gradient versus impact energy for each of the five segments as the impact energy was progressively increased. The potential gradient of a segment was

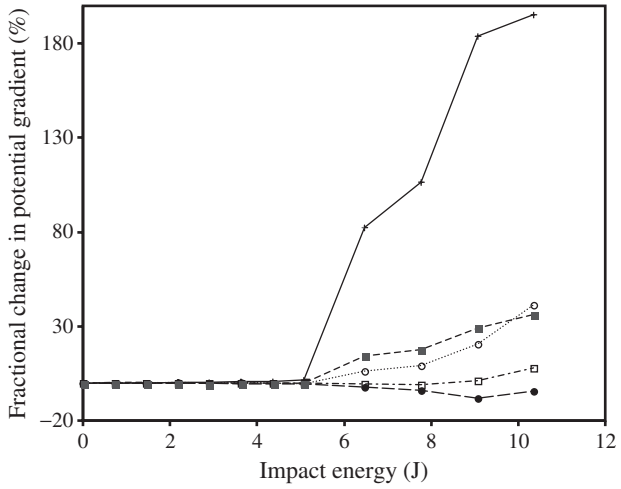

Figure 3. *Fractional change in potential gradient vs. impact energy for the 8-lamina composite and the configuration of Figure 1(a). □: A_1A_2, ○: A_2A_3, +: A_3A_4, ●: A_4A_5, ■: A_5A_6.*

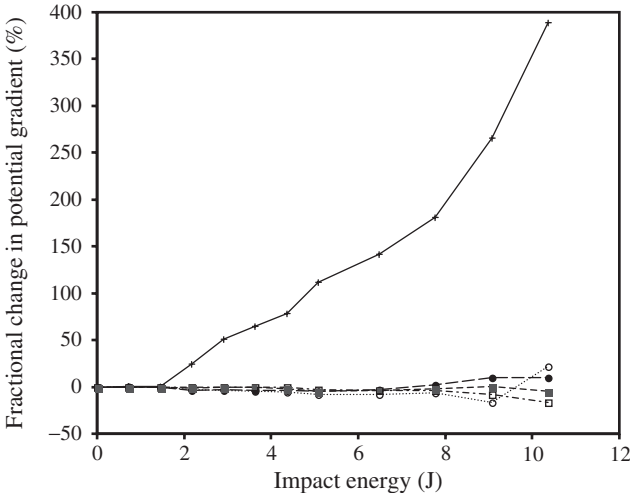

Figure 4. *Fractional change in potential gradient vs. impact energy for the 8-lamina composite and the configuration of Figure 1(b). □: B_1B_2, ○: B_2B_3, +: B_3B_4, ●: B_4B_5, ■: B_5B_6.*

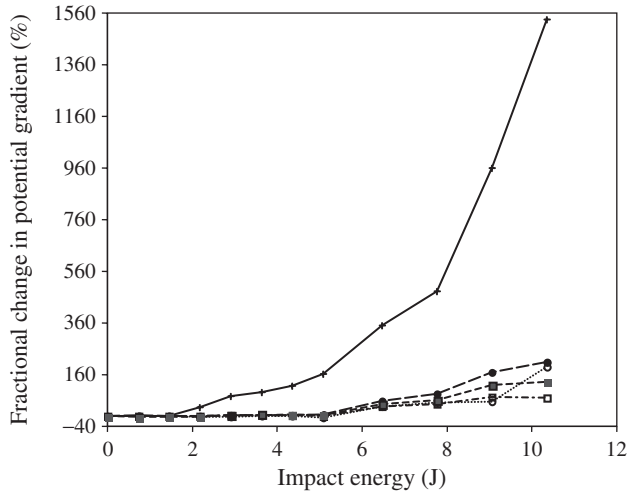

Figure 5. *Fractional change in potential gradient vs. impact energy for the 8-lamina composite and the configuration of Figure 1(c). □: B_1B_2, ○: B_2B_3, +: B_3B_4, ●: B_4B_5, ■: B_5B_6.*

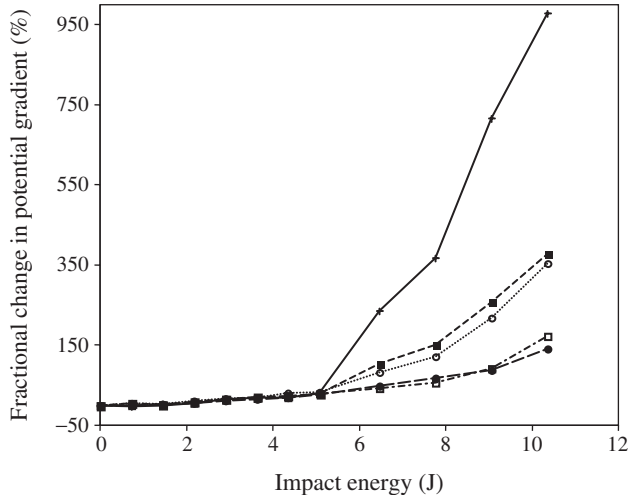

Figure 6. *Fractional change in potential gradient vs. impact energy for the 8-lamina composite and the configuration of Figure 1(d). □: A_1A_2, ○: A_2A_3, +: A_3A_4, ●: A_4A_5, ■: A_5A_6.*

obtained by dividing the potential drop along the whole length of the segment by the length of the segment.

Figures 3–6 all show that the potential gradient increased with increasing impact energy for the segment containing the point of impact, such that the increase started to be significant at an impact energy of 6.4 ± 1.3, 1.5 ± 0.4, 1.5 ± 0.4, and 6.4 ± 1.3 J for the cases of Figures 3–6, respectively. These four values were based on the data for the three specimens tested. The low values in the cases of Figures 4 and 5 (i.e., cases of Figure 1(b) and (c), respectively) compared to the values of the cases of Figures 3 and 6 (i.e., cases of Figure 1(a) and (d) respectively) suggest that the method is more sensitive to minor damage when the potential is measured at the bottom surface. The result is probably due to current path distortion resulting from the impact

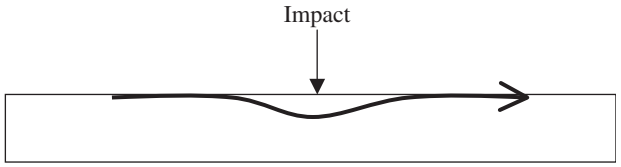

Figure 7. *Edge view of composite illustrating the current path distortion. The thick arrow indicates the current, which was applied to the top surface.*

at the top surface. The top current path (case of Figure 1(c)) is distorted (Figure 7) so that the current density at the bottom surface is enhanced. The bottom current path (case of Figure 1(b)) is distorted so that the current spreads less to the top part of the specimen, thereby enhancing the current density at the bottom surface. However, the result may also be due to residual stress relief in the region next to the heart of the damage, as the stress relief may decrease the local resistivity, thereby enhancing the local current density. The origin of the observed phenomenon is not completely understood.

For all the other segments in Figures 5 and 6, the potential gradient also increased with increasing impact energy, though the fractional increase was significantly less than that for the segment containing the point of impact. However, in Figures 3 and 4, for the segments not containing the point of impact, the potential either increased or slightly decreased as the impact energy increased.

The increase in potential gradient as the impact energy increased is due to the damage causing the resistance to increase. The slight decrease in potential gradient as the impact energy increased is consistent with the observation of Masson and Irving (2000). The origin of this decrease is not completely clear. However, it may be due to the distortion of the current path away from the surface to which the current was passed, as illustrated in Figure 7, which corresponds to the configurations in Figure 1(a) and (c). The current path distortion in Figure 7 causes less current on the top surface and hence a decrease in the potential gradient is measured at the top surface. On the other hand, the current applied at the bottom surface spreads to the top part of the specimen to a smaller extent when the top part suffers from impact damage. As a consequence, the current density at the top surface is decreased. For the segment containing the point of impact, the severity of the damage causes the effect of damage, which results in a resistance increase, to overshadow the effect of current path distortion. Thus, the effect of current path distortion could only be observed for segments not containing the point of impact.

Due to the distance separating the line of current application and the line of potential gradient measurement in the configurations of Figure 1(c) and (d), current path distortion essentially does not affect the

results in Figures 5 and 6, which therefore do not show the trend of the potential gradient decreasing with increasing impact energy. Although the decrease in the potential gradient with increasing impact energy in Figures 3 and 4 is a minor effect compared to the increase of the potential gradient with increasing impact energy, it complicates the interpretation of data for the purpose of damage sensing. The complication applies to segments not containing the point of impact. Therefore, the configurations of Figure 1(c) and (d), which correspond to the data of Figures 5 and 6 respectively, are more attractive for practical damage sensing than those of Figure 1(a) and (b), which correspond to the data of Figures 3 and 4, respectively.

For any of the segments, the fractional change in potential gradient is higher in Figures 5 and 6 than in Figures 3 and 4 for the same impact energy. It is particularly high in Figure 5 and particularly low in Figure 3, as shown for all three specimens. The high value for Figure 5 (case of Figure 1(c)) and the low value for Figure 3 (case of Figure 1(a)) are due to the current path distortion (Figure 7) causing the potential gradient measured at the top surface to decrease (due to decreased current density at the top surface) and causing the potential gradient measured at the bottom surface to increase (due to increased current density at the bottom surface). The particularly high values of the fractional change in potential gradient in Figure 5 give additional attraction for using the configurations of Figure 1(c).

It can be concluded that the potential method (Figure 1(c) and (d)) is superior to the resistance method (Figure 1(a) and (b)) for the 8-lamina composite. The superiority is in terms of the sensitivity for damage sensing and the simplicity of data interpretation.

24-Lamina Composite

Figures 8–11 show the results obtained for the 24-lamina composite using the configurations of Figure 1(a)–(d), respectively. The results in Figures 8 and 9 are qualitatively similar to those for the 8-lamina composite in Figures 3 and 4. It takes higher impact energy to attain a significant increase in potential gradient in Figures 8 and 9 than in Figures 3 and 4, due to the larger thickness of the 24-lamina composite compared to the 8-lamina composite.

The trend of the potential gradient decreasing with increasing impact energy for segments not containing the point of impact is more significant in Figures 8 and 9 than in Figures 3 and 4. In Figures 8 and 9, all segments not containing the point of impact exhibit this decreasing trend. In contrast, for Figures 3 and 4, not all segments that do not contain the point of impact exhibit this trend. This difference between the 8-lamina and

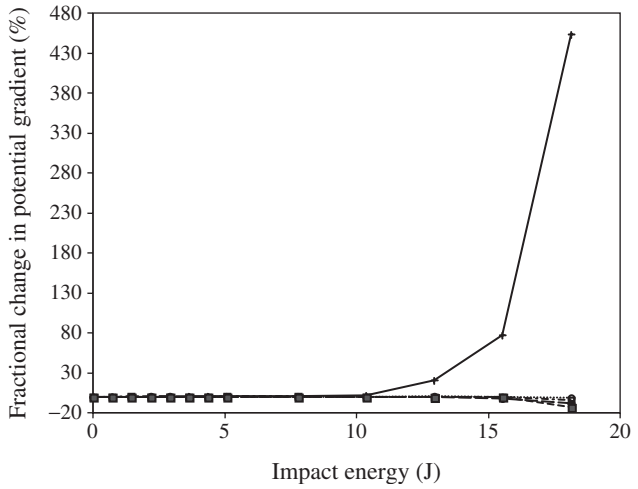

Figure 8. *Fractional change in potential gradient vs. impact energy for the 24-lamina composite and the configuration of Figure 1(a). □: A_1A_2, ○: A_2A_3, +: A_3A_4, ●: A_4A_5, ■: A_5A_6.*

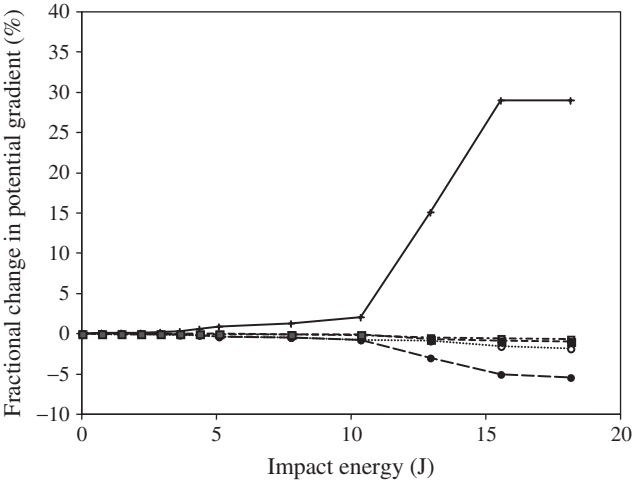

Figure 9. *Fractional change in potential gradient vs. impact energy for the 24-lamina composite and the configuration of Figure 1(b). □: B_1B_2, ○: B_2B_3, +: B_3B_4, ●: B_4B_5, ■: B_5B_6.*

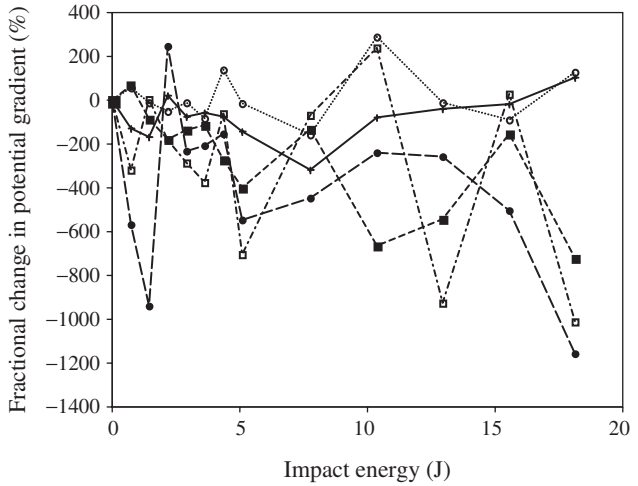

Figure 10. *Fractional change in potential gradient vs. impact energy for the 24-lamina composite and the configuration of Figure 1(c). □: B_1B_2, ○: B_2B_3, +: B_3B_4, ●: B_4B_5, ■: B_5B_6.*

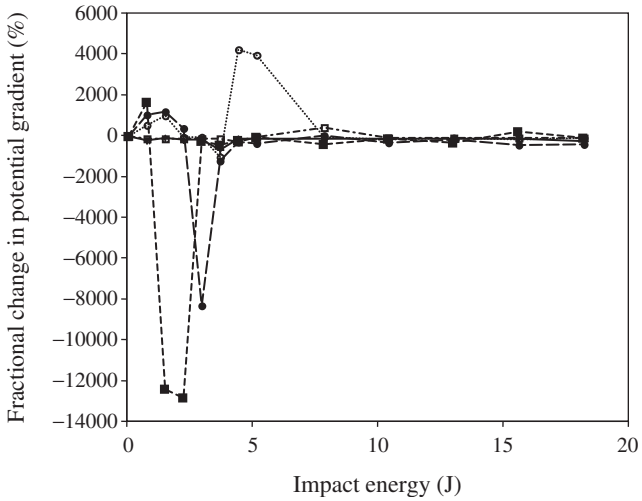

Figure 11. *Fractional change in potential gradient vs. impact energy for the 24-lamina composite and the configuration of Figure 1(d).* □: A_1A_2, ○: A_2A_3, +: A_3A_4, ●: A_4A_5, ■: A_5A_6.

24-lamina composites is consistent with the larger thickness of the 24-lamina composite and the consequent greater room for the current path distortion.

The results in Figures 10 and 11 are very different from those for the 8-lamina composite in Figures 5 and 6, as they show no systematic variation of the potential gradient with impact energy. This means that the configurations of Figures 1(c) and (d) do not work for the 24-lamina composite, though they work well for the 8-lamina composite. Therefore, for the 24-lamina composite, the configurations of Figure 1(a) and (b) are recommended.

The ineffectiveness of damage sensing using the configurations of Figure 1(c) and (d) for the 24-lamina composite is due to the large thickness of the 24-lamina composite and the consequent large resistance (in the through-thickness direction) between the current line and the potential gradient line. The greater the resistance, the lesser is the influence of the current on the potential gradient. A small influence results in non-systematic variation of the potential gradient.

Comparison of Figures 8 and 9 shows that, at the same impact energy, the fractional change in potential gradient is much higher in Figure 8 than in Figure 9. This means that the damage sensitivity is superior for the configuration of Figure 1(a) than that of Figure 1(b). However, an expanded view of Figures 8 and 9 (not shown) show that the ability to distinguish among different levels of damage for segments not containing the point of impact is superior for the configuration of Figure 1(b) that that of Figure 1(a). The superiority of the configuration of Figure 1(b) for sensing the level of minor damage is probably due to the slight degradation of the electrical contacts on the top surface (in the configuration of Figure 1(a)) upon impact on the top surface.

It can be concluded that the resistance method (Figure 1(a) and (b)) is superior to the potential method (Figure 1(c) and (d)) for the 24-lamina composite. In fact, the potential method does not work for the 24-lamina composite, due to the large distance of separation between the current line and the potential gradient line.

16-Lamina Composite

Results obtained for the 16-lamina composite are similar to those of the 24-lamina composite, in that the potential method does not work, while the resistance method works well.

CONCLUSION

The electrical resistance method and the electric potential method for composite damage selfsensing were compared for the case of the applied current direction and the measured potential gradient direction being parallel. In the potential method, these parallel directions are in different planes (one plane being the top surface of a laminate and the other plane being the bottom surface of the laminate). In the resistance method, these parallel directions are the same lines in the same plane. Each method was performed with the current at the top surface and with the current at the bottom surface, while impact was directed at the center of the top surface. The study was conducted on 8-lamina, 16-lamina, and 24-lamina composites.

Both resistance and potential methods were effective for damage sensing for the 8-lamina composite. For the 16-lamina and 24-lamina composites the resistance method was effective, whereas the potential method was not. This means that the potential method does not work when the distance of separation between the applied current line and the potential gradient line is excessive. A distance of 2.1 mm (16 laminae) in the through-thickness direction is excessive, whereas a distance of 1.0 mm (8 laminae) in this same direction is not.

For the 8-lamina composite, the potential method was superior to the resistance method, as shown by higher sensitivity for damage sensing and essential absence of the minor phenomenon of the potential gradient decreasing with increasing impact energy. In contrast, the resistance method was complicated by this minor phenomenon, which tended to occur for the segments not containing the point of impact. These aspects of superiortity of the potential method over the resistance method for the 8-lamina composite are explained in terms of the current path distortion resulting from the impact damage.

ACKNOWLEDGMENT

This work was supported in part by U.S. National Science Foundation.

REFERENCES

Abry, J.C., Bochard, S., Chateauminois, A., Salvia, M. and Giraud, G. 1999. "*In Situ* Detection of Damage in CFRP Laminates by Electrical Resistance Measurements," *Composites Science Technology*, 59(6):925–935.

Abry, J.C., Choi, Y.K., Chateauminois, A., Dalloz, B., Giraud, G. and Salvia, M. 2001. "*In-Situ* Monitoring of Damage in CFRP Laminates by Means of AC and DC Measurements," *Composites Science Technology*, 61(6):855–864.

Angelidis, N., Khemiri, N. and Irving, P.E. 2005. "Experimental and Finite Element Study of the Electrical Potential Technique for Damage Detection in CFRP Laminates," *Smart Materials and Structures*, 14:147–154.

Aoki, Y. and Byon, O-II. 2001. "Strain Sensor Output-based Health Monitoring of CFRP Structures by Using Localized Flexibility Method," In: Takashi Ishikawa and Sunao Sugimoto (eds), *Information and Innovation in Composites Technologies, Proceedings of the Japan International SAMPE Symposium*, SAMPE, Covina, CA, pp. 911–914.

Avier, M.J. and Clarke, M.P. 1995. "Experimental Techniques for the Investigation of the Effects of Impact Damage on Carbon Fiber Composites," *Composites Science and Technology*, 55(2):157–169.

Ceysson, O., Salvia, M. and Vincent, L. 1996. "Damage Mechanisms Characterisation of Carbon Fibre/Epoxy Composite Laminates by Both Electrical Resistance Measurements and Acoustic Emission Analysis," *Scripta Mater.*, 34(8):1273–1280.

Chu, Y.-W. and Yum, Y.-J. 2001. "Detection of Delamination in Graphite/Epoxy Composite by Electric Potential Method," In: *Proceedings – KORUS 2001, The 5th Korea–Russia International Symposium on Science and Technology, Section 5 – Mechanics and Automotive Engineering*, IEEE, Piscataway, NJ, pp. 240–242.

Chung, D.D.L. and Wang, S. 2003. "Self-Sensing of Damage and Strain in Carbon Fiber Polymer-Matrix Structural Composites by Electrical Resistance Measurement," *Polymers and Polymer Composites*, 11(7):515–525.

Chung, K. and Seferis, J.C. 1998. "Investigation of the Thermal Aging Behavior of Cyanate Ester/Carbon Fiber Composite," In: *International SAMPE Symposium and Exhibition, 43rd Materials and Process Affordability – Keys to the Future*, Vol. 1, SAMPE, Covina, CA, pp. 87–393.

Clerico, M., Ruvinetti, G., Cipri, F. and Pelosi, M. 1989. "Analysis of Impact Damage and Residual Static Strength in Improved CFRP (Carbon Fiber-Reinforced Plastics)," *International Journal of Materials and Products Technology*, 4(1):61–70.

de Freitas, M., Silva, A. and Reis, L. 2000. "Numerical Evaluation of Failure Mechanisms on Composite Specimens Subjected to Impact Loading," *Compos. Part B – Eng.*, 31(3):199–207.

Haque, A. and Raju, P.K. 1998. "Monitoring Fatigue Damage in Carbon Fiber Composites Using an Acoustic Impact Technique," *Materials Evaluation*, 56(6):765–770.

Irving, P.E. and Thiagarajan, C. 1998. "Fatigue Damage Characterization in Carbon Fibre Composite Materials using an Electrical Potential Technique," *Smart Materials and Structures*, 7:456–466.

Kaddour, A.S., Al-Salehi, A.R., Al-Hassani, S.T.S. and Hinton, M.J. 1994. "Electrical Resistance Measurement Technique for Detecting Failure in CFRP Materials at High Strain Rates," *Composites Science and Technology*, 51(3):377–385.

Kupke, M., Schulte, K. and Schüler, R. 2001. "Non-Destructive Testing of FRP by D.C. and A.C. Electrical Methods," *Composites Science and Technology*, 61:837–847.

Masson, L.C. and Irving, P.E. 2000. "Comparison of Experimental and Simulation Studies of Location of Impact Damage in Polymer Composites using Electrical Potential Techniques," In: Pierre François Gobin and Clifford M. Friend (eds), *Proceedings of SPIE, 5th European Conference on Smart Structures and Materials*, Vol. 4073, SPIE, Bellingham, WA, pp. 182–193.

Mei, Z., Guerrero, V.H., Kowalik, D.P. and Chung, D.D.L. 2002. "Mechanical Damage and Strain in Carbon Fiber Thermoplastic-Matrix Composite, Sensed by Electrical Resistivity Measurement," *Polymer Composites*, 23(3):425–432.

Muto, N., Yanagida, H., Nakatsuji, T., Sugita, M., Ohtsuka, Y. and Arai, Y. 1992. "Design of Intelligent Materials with Self-Diagnosing Function for Preventing Fatal Fracture," *Smart Materials and Structures*, 1:324–329.

Muto, N., Yanagida, H., Nakatsuji, T., Sugita, M., Ohtsuka, Y., Arai, Y. and Saito, C. 1995. "Materials Design of CFGFRP-Reinforced Concretes with Diagnosing Function for Preventing Fatal Fracture," *Advanced Composite Materials*, 4(4):297–308.

Prabhakaran, R. 1990. "Damage Assessment through Electrical Resistance Measurement in Graphite Fiber-Reinforced Composites," *Experimental Techniques*, 14(1):16–20.

Rose, J.L., Rajana, K.M. and Barshinger, J.N. 1996. "Guided Waves for Composite Patch Repair of Aging Aircraft," *Review of Progress in Quantitative Nondestructive Evaluation*, 15B:1291–1298.

Schulte, K. 1993. "Damage Monitoring in Polymer Matrix Structures," *Journal de Physique III Colloque C7*, 3:1629–1636.

Shin, E.E., Jurek, R., Drzal, L.T., Morgan, R.J., Choi, J.-K. and Lee, A. 1995. "Durability and Critical Fundamental Aging Mechanisms of High Temperature Polymer Matrix Carbon Fiber Composites: Part 1," In: *69th Proceedings of the ASME Materials Division, American Society of Mechanical Engineers*, Vol. 1, ASME International, New York, NY, pp. 183–189.

Shin, E.E., Morgan, R.J., Wilenski, M., Zhou, J., Lincoln, J. and Drzal, L.T. 1996. "The Effects of Processing Conditions and Service Environmental Exposures on High-Temperature Polymer Matrix Carbon Fiber Composites," In: *International SAMPE Technical Conference, 28th Technology Transfer in a Global Community*, SAMPE, Covina, CA, pp. 225–235.

Sjogren, A., Krasnikovs, A. and Varna, J. 2001. "Experimental Determination of Elastic Properties of Impact Damage in Carbon Fibre/Epoxy Laminates," *Composites Part A – Applied Science and Manufacturing*, 32(9):1237–1242.

Staszewski, W.J., Pierce, S.G., Worden, K. and Culshaw, B. 1999. "Cross-wavelet Analysis for Lamb Wave Damage Detection in Composite Materials Using Optical Fibers," *Key Engineering Materials*, 167–168.

Sugita, M., Yanagida, H. and Muto, N. 1995. "Materials Design for Self-Diagnosis of Fracture in CFGFRP Composite Reinforcement," *Smart Materials Structures*, 4(1A):A52–A57.

Todoroki, A., Kobayashi, H. and Matuura, K. 1995. "Application of Electric Potential Method to Smart Composite Structures for Detecting Delamination," *JSME International Journal Series A – Solid Mechanics and Material Engineering*, 38(4):524–530.

Todoroki, A., Tanaka, Y. and Shimamura, Y. 2004. "Multi-Prove Electric Potential Change Method for Delamination Monitoring of Graphite/Epoxy Composite Plates using Normalized Response Surfaces," *Composite Science Technology*, 64(5):749–758.

Verma, R.K., Kander, R.G. and Hsiao, B.S. 1994. "Acoustic Emission Monitoring of Damage using High Amplitude Gains in Carbon Fiber Reinforced Poly(Ether Ketone Ketone)," *Journal of Material Science Letters*, 13(6):438–442.

Wang, X. and Chung, D.D.L. 1999. "Fiber Breakage in Polymer-Matrix Composite during Static and Dynamic Loading, Studied by Electrical Resistance Measurement," *Journal of Materials Research,* 14(11):4224–4229.

Wang, S. and Chung, D.D.L. 2002. "Mechanical Damage in Carbon Fiber Polymer-Matrix Composite, Studied by Electrical Resistance Measurement," *Composite Interfaces*, 9(1):51–60.

Wang, S., Shui, X., Fu, X. and Chung, D.D.L. 1998a. "Early Fatigue Damage in Carbon Fiber Composites, Observed by Electrical

Resistance Measurement," *Journal of Materials Science*, 33(15):3875–3884.

Wang, X., Fu, X. and Chung, D.D.L. 1998b. "Electromechanical Study of Carbon Fiber Composites," *Journal of Materials Research,* 13(11):3081–3092.

Wang, X, Wang, S. and Chung, D.D.L. 1999. "Sensing Damage in Carbon Fiber and Its Polymer-Matrix and Carbon-Matrix Composites by Electrical Resistance Measurement," *Journal of Materials Research*, 34(11):2703–2714.

Wang, S., Mei, Z. and Chung, D.D.L. 2001. "Interlaminar Damage in Carbon Fiber Polymer-Matrix Composites, Studied by Electrical Resistance Measurement," *International Journal of Adhesion and Adhesives*, 21(ER6):465–471.

Wang, S., Kowalik, D.P. and Chung, D.D.L. 2004. "Self-Sensing Attained in Carbon Fiber Polymer-Matrix Structural Composites by using the Interlaminar Interface as a Sensor," *Smart Materials and Structures*, 13(3):570–592.

Wang, S., Chung, D.D.L. and Chung, J.H. (2005). "Impact Damage of Carbon Fiber Polymer-Matrix Composites, Monitored by Electrical Resistance Measurement," *Composites: Part A*, 36:1707–1715.

Wang, S., Chung, D.D.L. and Chung, J.H. (a). "Method of Sensing Impact Damage in Carbon Fiber Polymer-Matrix Composite by Electrical Resistance Measurement," *Journal of Materials Science* (in press).

Wang, S., Chung, D.D.L. and Chung, J.H. (b). "Self-Sensing of Damage in Carbon Fiber Polymer-Matrix Composite by Measurement of the Electrical Resistance or Potential Away from the Damaged Region," *Journal of Materials Science* (in press).

Wolterman, R.L., Kennedy, J.M. and Farley, G.L. 1993. "Fatigue Damage in Thick, Cross-Ply Laminates with a Center Hole," ASTM Special Technical Publication, STP 1156, *Composite Materials: Fatigue and Fracture*, 4:473–490.

Yoshitake, K., Shiba, K., Suzuki, M., Sugita, M. and Okuhara, Y. 2004. "Damage Evaluation for Concrete Structures using Fiber Reinforced Composites as Self-Diagnosis Materials," In: Eric Udd and Daniele Inaudi (eds), *Smart Structures and Materials 2004: Smart Sensor Technology and Measurement Systems, Proceedings of SPIE*, Vol. 5384, SPIE, Bellingham, WA, pp. 89–97.